ELSEVIER

Thermochimica Acta 314 (1998) 35–53

thermochimica acta

Binary phase diagrams of tellurium and post-transitional elements (IB, IIB, IIIB, IVB, VB, VIB)

Yves Feutelais*, Bernard Legendre

Laboratoire de Chimie Physique Minérale et Bioinorganique, EA 401 5, rue J.-B. Clément, F-92296 Châtenay-Malabry, France

Received 22 October 1997; accepted 19 November 1997

1. Introduction

In Table 1, we give some examples of practical applications for tellurium based alloys. Elaboration of new materials always leads to more efficient results in searching more and more complex alloys (containing n elements with $n \geq 3$). From an experimental point of view, the study of stability of such phases needs a lot of experiments with the effect of increasing drastically the cost of the project. Another way, which seems faster and less expensive, is to use thermodynamic evaluation of the boundary systems to calculate, according to reasonable assumptions, the phase diagram of interest. Experimental verification, made on particular compositions allows to refine the modelization.

Such a procedure needs the knowledge of the Gibbs functions of all phases encountered in the system. Today the thermodynamic functions of pure elements are available under the form of a database [1]. As access to the thermodynamic knowledge of ternary and quaternary alloys the previous determination of the Gibbs functions of the binary systems is needed therefore, we will present below a review of the binary systems including tellurium and a post-transitional element.

Considering these elements, only six telluride systems have not yet been evaluated thermodynamically: Cu–Te, Ag–Te, As–Te and Bi–Te. As shown in Table 2, the optimization of two other systems (Si–Te, Ge–Te) is in progress.

2. Systems Cu–, Ag–, Au–Te

2.1. System Cu–Te

This binary is obviously the most complicated tellurium system of the post-transitional elements, this is the reason why only a graphical description is proposed. It is actually impossible to realise an optimization, because some data are conflicting, and other are missing, especially for the definition of the phase fields.

An assessment has been proposed [2] and the diagram is reported Fig. 1(a) and (b). The Cu–Te diagram is characterized by a miscibility gap with a monotectic reaction:

$$L_2 = L_1 + Cu_2Te, \quad T = 1092^\circ C$$

a eutectic in the Cu rich part exists:

$$L_1 = Cu + Cu_2Te, \quad T = 1050^\circ C$$

Three groups of solid compounds exist: $Cu_{2-x}Te$, $Cu_{3-x}Te$ and CuTe. They present a lot of phase transitions.

*Corresponding author. E-mail: yves.feutelais@cep.u-psud.fr

PII S0040-6031(97)00479-6

Table 1
Examples of applications of some tellurium based alloys

System	Practical application	Elaboration needs
Hg–Cd–Te	Electronic devices	
Pb–Te Bi–Sb–Te	Refrigerating materials	Phase diagram
Cd–Te	Photovoltaic detectors optical crystals	Knowledge
Zn–Te	Optical devices	
Sb–Se–Te, In–Sb–Te Au–Ge–Sn–Te Ag–Tl–Ge–Sb–Te	Phase change media for optical recording	(T–X), (P–T–X)

Table 2
Literature references of optimized systems

I	II	III	IV	V	VI
		Al	Si		
		[15]	[in progress]		
Cu	Zn	Ga	Ge	As	Se
	[12]	[18,19]	[in progress]		[65]
Ag	Cd	In	Sn	Sb	
	[69]	[15]	[45–47]	[52]	
Au	Hg	Tl	Pb	Bi	
[9]	[69]	[27,29]	[68]		

Table 3
Range of existence of the phases in the Cu–Te phase diagram

Phases	Range of existence	
	Composition in at.% Te	Temperature in °C
a	33.5–33.6	<277
b	34.4–34.9	<177
c	34.1–35.0	170–320
d	35.2–35.6	<250
e	35.2–36.2	250–342
f	35.8–36.2	<277
g	35.4–35.9	227–265
h	33.7–34.0	270–317
j	33.7–35.5	300–362
k	33.5–36.0	352–574
m	33.5–36.2	357–1140
n	40.0–41.1	<140
p	40.0–41.1	360–650
q	40.0–41.1	650–790

The range of existence of these phases and a compatible arrangement with the phase rule has been proposed by [3] and has been slightly modified by [2] (Fig. 1(b)). Even though a lot of works of quality have been devoted to this system, it is not actually possible to get an optimization of this system.

Table 3 gives the range of existence of the different phases. In Table 4 are given the generally accepted invariants.

2.2. System Ag–Te

The general shape of this diagram is close to Cu–Te but simpler. An assessment has been proposed by [2]. The characteristic of this binary phase diagram is the existence of a liquid–liquid demixtion in the Ag rich part, and three binary compounds, all of them present phase transitions.

The construction of the equilibria between the solid phases is due to [4]. The phase diagram presents the reactions given in Table 5.

The full diagram is presented in Fig. 1(c). The heat of mixing has been measured by calorimetry by [5–8], the integral enthalpy of mixing shows a sharp minimum at 33 mol% tellurium (−20 kJ/mol) and is less negative when the temperature increases. An optimization of this system is in progress.

2.3. System Au–Te

This system is quite different from Cu–Te and Ag–Te, it has no liquid–liquid demixtion though the shape of the liquidus in the gold rich part is rather flat, which indicates a tendency to immiscibility. The only existing compound is $AuTe_2$ with a low melting point (463.3°C) and it does not present a solid solution like Cu_2Te and Ag_2Te, high melting points and solid solutions. The heat of mixing in the liquid state is not so high than for Ag–Te and Cu–Te. Apparently the liquid is not associated. This diagram has been optimized by [9] (Fig. 1(d)). Invariant reactions are given in Table 6.

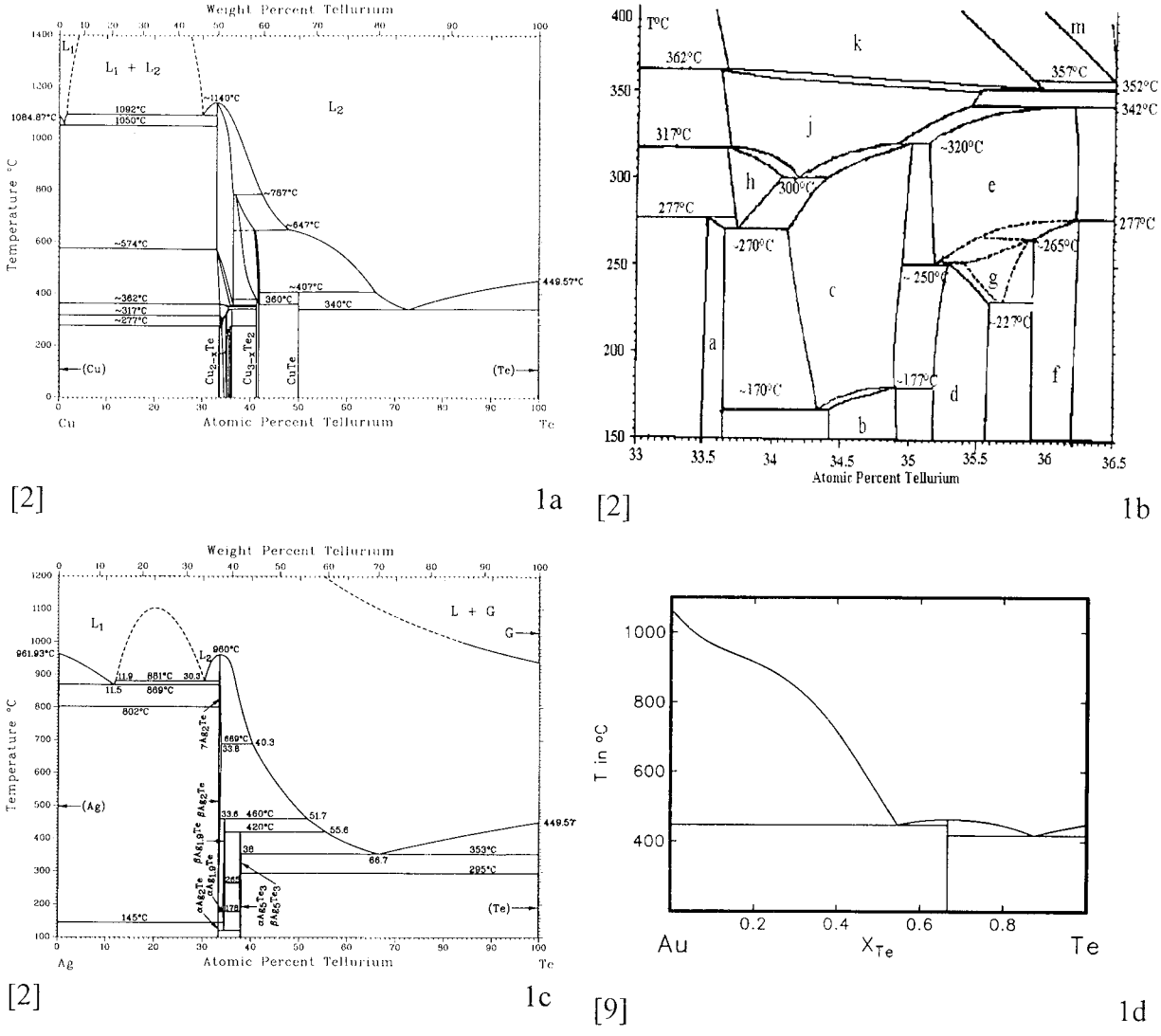

Fig. 1. Cu–, Ag–, Au–Te phase diagram ((a)–(c): courtesy of American Institute of Metals).

Table 4
Invariant reactions in the system Cu–Te

Reaction	T in °C	Composition of the respective phases in at.% Te		
$L_2=L_1+Cu_2Te$	1092 [2,3]	0.300	0.020	0.333
$L_1=Cu+Cu_2Te$	1050 [2,3]	0.015	0.000	0.333
Cu_2Te (L)=Cu_2Te (S)	1140 [2,3]	0.333	0.333	
$L+Cu_{2-x}Te$ (m)=$Cu_{3-x}Te_2$ (q)	787 [2,3]	0.430	0.37	0.38
$L+Cu_{3-x}Te_2$ (p)=CuTe	407 [2,3]	0.660	0.420	0.500
L=CuTe+Te	340 [2,3]	0.730	0.500	1.000

Table 5
Invariant reactions in the system Ag–Te

Reaction	T in °C	Composition of the respective phases in at.% Te		
$L_2=L_1+Ag_2Te\gamma$	881 [2]	0.303	0.119	0.333
$L_1=Ag+Ag_2Te\gamma$	869 [2]	0.115	0.000	0.333
$Ag+Ag_2Te\gamma=Ag_2Te\beta$	802 [2]	0.000	0.333	0.336
Ag_2Te (L)$=Ag_2Te\gamma$	960 [2]	0.333	0.333	
$Ag_2Te\gamma=Ag_2Te\beta+L$	689 [2]	0.338	0.337	0.403
$Ag_2Te\beta+L=Ag_{1.9}Te\beta$	460 [2]	0.336	0.517	0.345
$Ag_{1.9}Te\beta+L=Ag_5Te_3\beta$	420 [2]	0.347	0.556	0.378
$L=Ag_5Te_3\beta+Te$	353 [2]	0.667	0.380	1.000
$Ag_5Te_3\beta+Te=Ag_5Te_3\alpha$	295 [2]	0.379	1.000	0.380
$Ag_5Te_3\beta=Ag_5Te_3\alpha+Ag_{1.9}Te\beta$	265 [2]	0.369	0.370	0.350
$Ag_{1.9}Te\beta+Ag_2Te\beta=Ag_{1.9}Te\alpha$	178 [2]			
	182 [4]	0.343	0.333	0.342
$Ag_{1.9}Te\beta=Ag_5Te_3\alpha+Ag_2Te\alpha$	178 [2]			
	178 [4]	0.349	0.370	0.348
$Ag_2Te\beta=Ag_2Te\alpha$	145 [2]	0.333	0.333	
$Ag_{1.9}Te\alpha=Ag_5Te_3\alpha+Ag_2Te\alpha$	120 [2]	0.345	0.378	0.333
	120 [4]	0.345	0.370	0.333

Table 6
Invariant reactions in the Au–Te system

Reaction	T in °C	Composition of the respective phases in at.% Te		
$L=Au+AuTe_2$	447.8 [9]	0.545	0.00	0.667
	447 [70]	0.53	0.000	0.667
$AuTe_2$ (S)$=AuTe_2$ (L)	462.9 [9]	0.667	0.667	
	464 [70]	0.667	0.667	
$L=AuTe_2+Te$	416.9 [9]	0.874	0.667	1.000
	416 [70]	0.88	0.667	1.000

3. Systems Zn–, Cd–, Hg–Te

Their phase diagrams and invariant reactions are given in Fig. 2(a)–(c) and Table 7. The three systems, which look very similar, are characterized by an equiatomic compound with congruent melting. The melting temperature is decreasing from ZnTe (1297°C) to CdTe (1095°C) and HgTe (673°C). In the thermodynamic evaluation of the three systems, the liquid has been successfully described with the association model [10,11]. The shape of the liquidus curve between the metallic element and the com-pound is directly correlated to the enthalpic coefficient ($K_{\text{met,associate}}$) of the interaction parameter between the metal and the associate. A positive interaction is the result of repulsion between the metallic element and the associate. If the repulsion is higher the enthalpic coefficient is more positive (Table 8).

Another characteristic of these systems is the relative low boiling point of the pure elements in comparison with the melting point of the intermediate compound. Calculations of the phase diagram at different pressures made for Zn–Te [12] and Cd–Te [13] are given in Fig. 3. According to the analytical description of the phases given in these works, the effect of pressure acts only on the Gibbs energy of the gas phases assumed to behave as ideal mixtures. At atmospheric pressure, interference of gas phase with solid

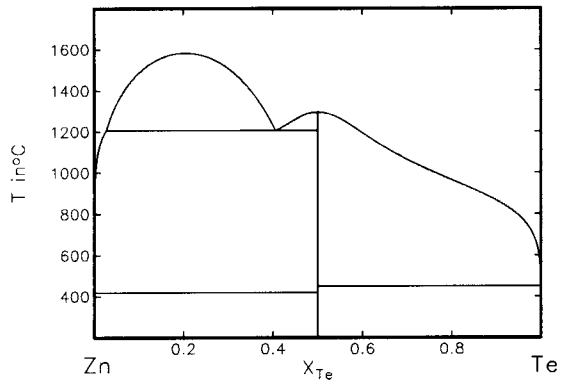

[12] 2a

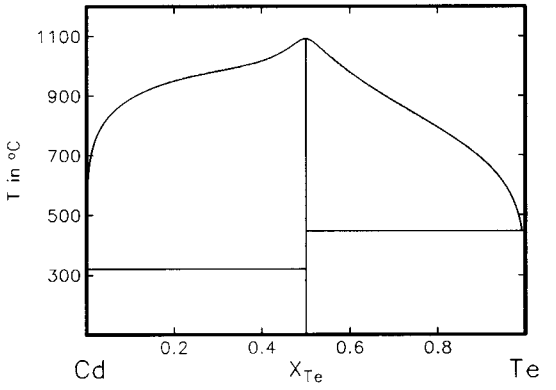

[69] 2b

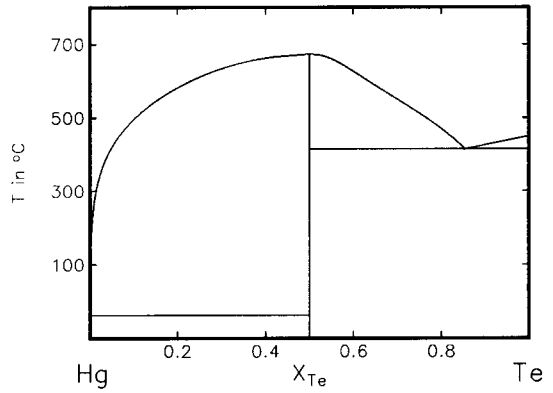

[69] 2c

Fig. 2. Zn–, Cd–, Hg–Te phase diagram.

and/or liquid phases is present in both systems. Furthermore, at 1 bar, the compound ZnTe decomposes before melting. Thus the use of conventional DSC and DTA apparatus, which do not allow control of pressure may explain the differences observed in the phase diagram data. Increasing pressure raises the boiling point temperatures with the consequence of separation of the gas phase from the condensed phases. A thermodynamic peculiarity can be observed at a pressure of 5.64 bars in the Cd–Te phase diagram: an invariant point where the three phases $G_{(\text{rich in Cd})}+L \Leftrightarrow L+CdTe$ are in equilibrium in which liquid L has the same composition on both sides.

4. Systems Al–, Ga–, In–, Tl–Te

4.1. System Al–Te

This system has been assessed by [2]. It is mainly based on the data of [14] and presents a compound Al_2Te_3 with a congruent melting point at 895°C and a liquid–liquid miscibility gap, with a maximum at 957°C. The invariant reactions are given in Table 9.

This system has been optimized by [15] assuming that strong interactions exist in the liquid. The liquidus is described with a model proposed by [16]. Al_2Te_3 is supposed to be stoichiometric. The phase diagram is presented in Fig. 4(a).

Table 7
Invariant reactions in the systems Zn–Te, Cd–Te and Hg–Te

Reaction	T in °C	Composition of the respective phases in at.% Te		
L_1=Zn+ZnTe	≈419.58 [2]	degenerate	0.000	0.500
	419.6 [12]	degenerate	0.000	0.500
L_2=L_1+ZnTe	1215 [2]	0.346	0.05	0.500
	1207.0 [12]	0.406	0.028	0.500
ZnTe (L)=ZnTe (S)	1300 [2]	0.500	0.500	
	1297 [12]	0.500	0.500	
L_2=ZnTe+Te	449 [2]	0.9973	0.500	1.000
	449.4 [12]	degenerate	0.500	1.000
L=Cd+CdTe	321 [2]	degenerate	0.000	0.500
	321.1 [69]	degenerate	0.000	0.500
CdTe (L)=CdTe (S)	1098 [2]	0.500	0.500	
	1095 [69]	0.500	0.500	
L=CdTe+Te	446.2 [2]	0.9861	0.500	1.000
	447.0 [69]	0.9900	0.500	1.000
L=Hg+HgTe	−38.83 [2]	degenerate	0.000	0.500
	−38.8 [69]	degenerate	0.000	0.500
HgTe (L)=HgTe (S)	670 [2]	0.500	0.500	
	672.8 [69]	0.500	0.500	
L=HgTe+Te	410.9 [2]	0.99	0.500	1.000
	413.3 [69]	0.854	0.500	1.000

Table 8
Otimized enthalpic interaction coefficient metal-associate

Zn–Te	Cd–Te	Hg–Te
$K_{Zn,ZnTe}$=71495.73 J/mol	$K_{Cd,CdTe}$=50245.05 J/mol	$K_{Hg,HgTe}$=−6986.97 J/mol
[12]	[69]	[69]
Miscibility gap	Tendency to demixing	No tendency to demixing

Table 9
Invariant reactions in the system Al–Te

Reaction	T in °C	Composition of the respective phases in at.% Te		
L_2=L_1+AL_2Te_3	843±5 [2]	0.54	0.080	0.600
	843 [15]	0.525	0.120	0.600
L_1=Al+AL_2Te_3	651±2 [2]	0.015	0.000	0.600
	646 [15]	0.029	0.000	0.600
AL_2Te_3 (L)=AL_2Te_3 (S)	895 [2]	0.600	0.600	
	887 [15]	0.600	0.600	
L_2=Te+AL_2Te_3	432±2 [2]	0.890	1.000	0.600

4.2. System Ga–Te

An assessed phase diagram (Fig. 4(b)) is proposed in [2], four stoichiometric compounds are observed. GaTe and Ga_2Te_3 with congruent melting points at 835°C and 798°C, Ga_3Te_4 with a peritectic decomposition at 784°C and Ga_2Te_5 between 407°C and 484°C. Furthermore this diagram has a miscibility gap induced by a monotectic reaction at 747°C and a critical point at 769°C in the Ga-rich side.

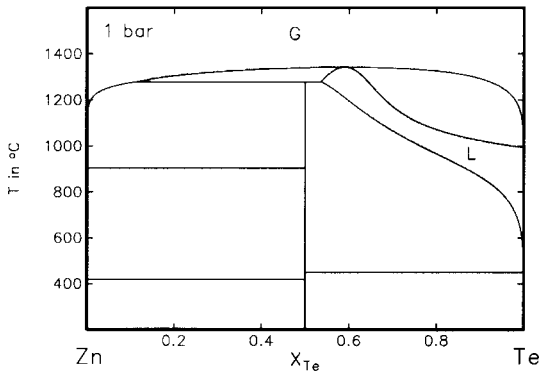

3a

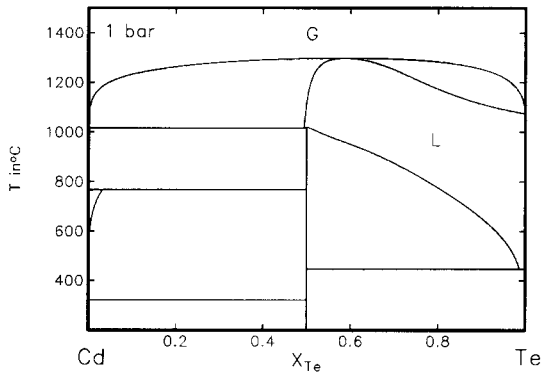

3d

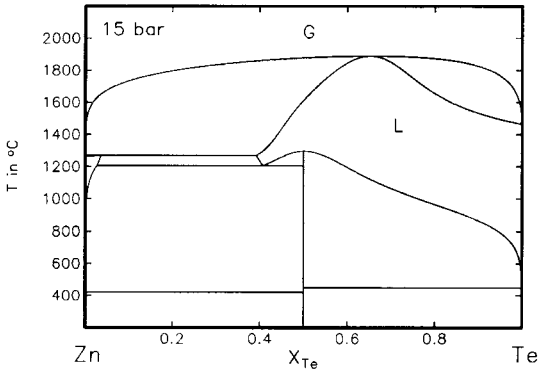

3b

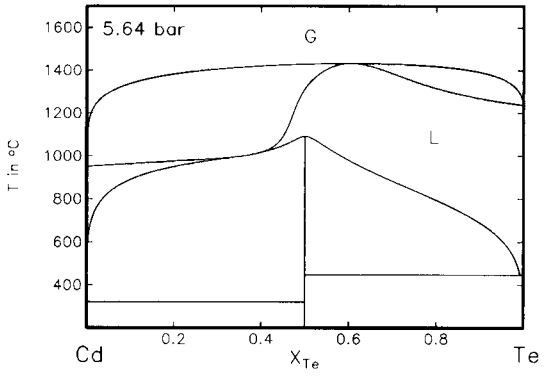

3e

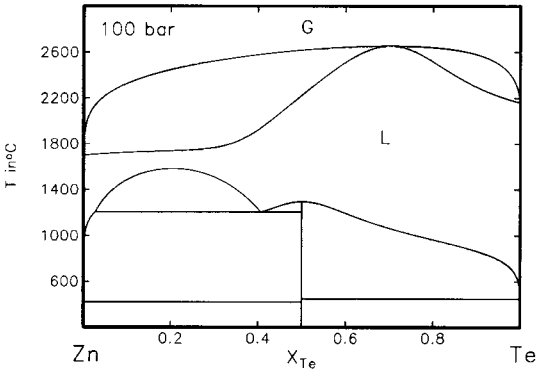

[12] 3c

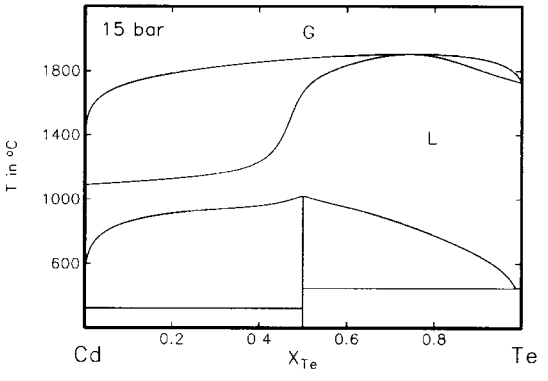

[13] 3f

Fig. 3. Zn–Te and Cd–Te phase diagram at different pressures.

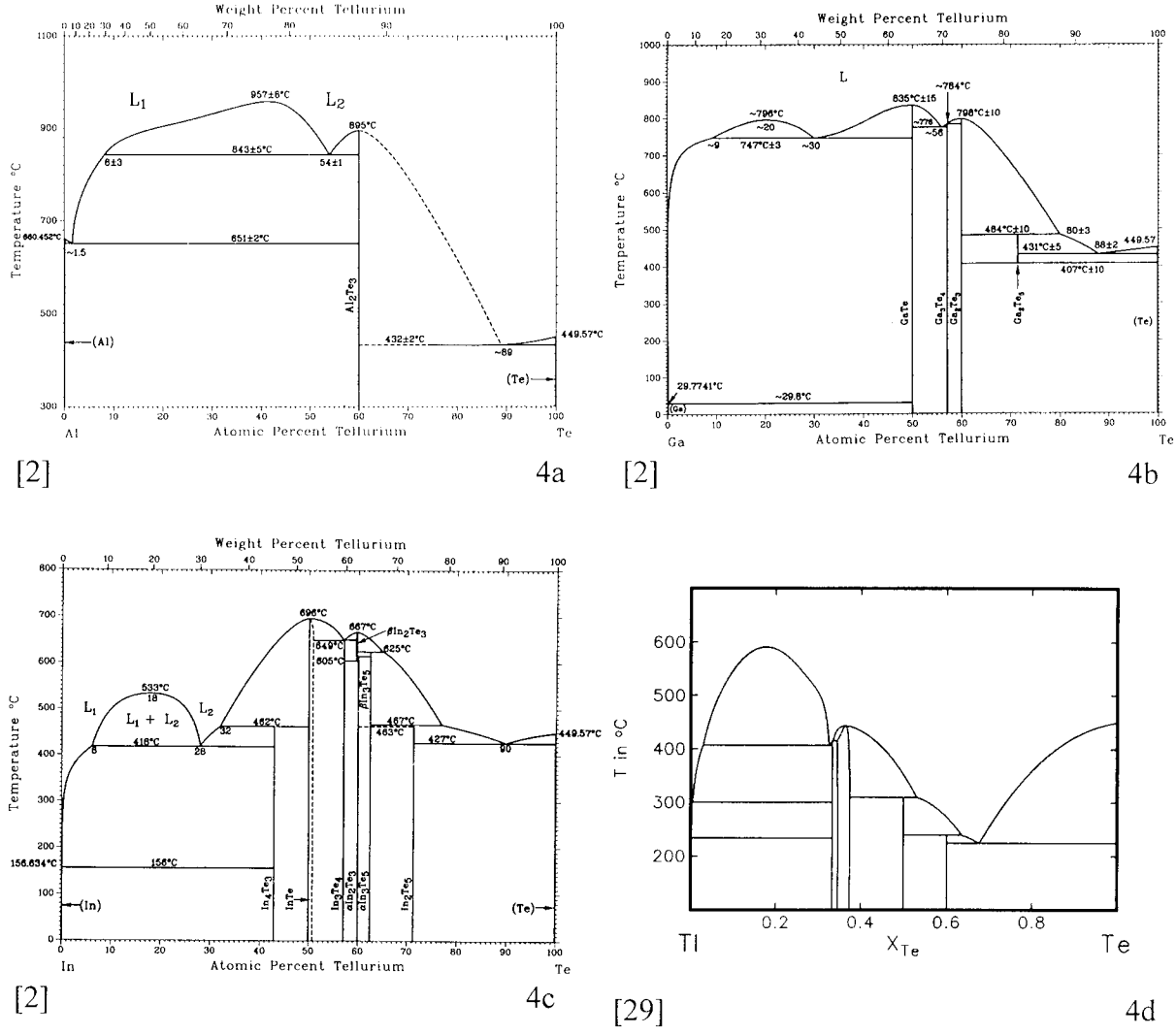

Fig. 4. Al–, Ga–, In–Te phase diagram ((a)–(c): courtesy of American Institute of Metals).

These conclusions are mainly based on the experimental work of [17]. An optimization has been performed by [18] using the association model for the liquid, this choice is justified by a strong negative enthalpy of mixing becoming less negative when the temperature increases.

Another optimization is proposed by [19], using Hillert's model [16]. More recently [20] proposed a phase diagram with only three intermediate compounds: GaTe, Ga_2Te_3 and Ga_2Te_5 for which no decomposition has been observed at 405°C. The different reactions are presented in Table 10.

4.3. System In–Te

An assessment is proposed by H. Okamoto [2], the following compounds are given:

In_4Te	non-congruent
InTe	congruent melting point at 696°C
In_3Te_4	non-congruent
In_2Te_3	congruent transition to β In_2Te_3 at 620°C
β-In_2Te_3	congruent melting point at 667°C
α-In_3Te_5	possible transition to β In_3Te_5 at 463°C
β-In_3Te_5	non-congruent

Table 10
Invariant reactions in the system Ga–Te

Reaction	T in °C	Composition of the respective phases in at.% Te		
L=Ga+GaTe or L+GaTe=Ga	[2,18,19]	degenerate	0.000	0.500
	≈29.8[a] [2]	degenerate	0.500	0.000
L_2=L_1+GaTe	747 [2]	0.300	0.090	0.500
	757.3 [18]	0.3624	0.1120	0.500
	742 [19]	0.302	0.088	0.500
	747 [20]	0.295	0.075	0.500
GaTe (L)=GaTe (S)	835±15 [2]	0.500	0.500	
	851.0 [18]	0.500	0.500	
	834 [19]	0.500	0.500	
L = GaTe+Ga_3Te_4	776 [2]	0.560	0.500	0.571
	774.4 [18]	0.5487	0.500	0.571
	788 [19]	0.561	0.500	0.571
L+Ga_2Te_3=Ga_3Te_4	784 [2]	0.571	0.600	0.571
	787.0 [18]	0.5656	0.600	0.571
	790 [19]	0.570	0.600	0.571
L=GaTe+Ga_2Te_3	787 [20]	0.570	0.500	0.600
Ga_2Te_3 (L)=Ga_2Te_3 (S)	798±10 [2]	0.600	0.600	
	806.0 [18]	0.600	0.600	
	806 [19]	0.600	0.600	
L+Ga_2Te_3=Ga_2Te_5	484 [2]	0.800	0.600	0.714
	488.3 [18]	0.8625	0.600	0.714
	488 [19]	0.862	0.600	0.714
	484 [20]	0.800	0.600	0.714
L=Ga_2Te_5+Te	431 [2]	0.880	0.714	1.000
	443.7 [18]	0.9496	0.714	1.000
	430 [19]	0.937	0.714	1.000
	430 [20]	0.900	0.714	1.000
Ga_2Te_5=Ga_2Te_3+Te	407 [2]	0.714	0.600	1.000
	405.9 [18]	0.714	0.600	1.000
	404 [19]	0.714	0.600	1.000

[a] The difference of temperature between the melting point of gallium and the invariant reaction is so weak that it is impossible to distinguish between a eutectic and the peritectic reaction.

Only the structures of In_4Te_3, InTe, In_2Te_5 and In_3Te_4 have been solved with monocrystals. In_3Te_4 has been obtained by high pressure preparation.

[15] has proposed an optimization in which the following phases are retained: In_9Te_7, InTe, In_3Te_4, $In_2Te_3\alpha$, $In_2Te_3\beta$, In_3Te_5 and In_2Te_5. The main difference with [2] is on the formula of In_4Te_3 or In_9Te_7 and the transition α–β of In_3Te_5 which is not taken into account in [15] and could be an order–disorder transition in [2].

According to the crystallographic study of [21], the formula is In_4Te_3. Invariant reactions are presented in Table 11.

Many calorimetric experiments have been performed [22–25] showing a strong temperature dependence in the liquid state, the minimum value is: -37 kJ mol^{-1} for x_{Te}=0.575 at 714°C and -29 kJ mol^{-1} at 1067°C.

This justifies the choice of Hillert's model by [15]. The phase diagram is presented in Fig. 4(c).

4.4. System Tl–Te

Much work has been devoted to thallium–tellurium alloys. Hall effect, electrical conductivity, thermoemf, density and viscosity measurements reveal some peculiar behaviour for x_{Te}=0.333. Concentration dependence of the Knights shifts and magnetic relaxation rate enhancements as well as heats of mixing

Table 11
Invariant reactions in the system In–Te

Reaction	T in °C	Composition of the respective phases in at.% Te		
$L=In+In_4Te_3$	156 [2]	degenerate	0.000	0.429
	156 [15]	degenerate	0.000	0.429
$L_2=L_1+In_4Te_3$	418 [2]	0.280	0.060	0.429
	426 [15]	0.260	0.060	0.429
$L+InTe=In_4Te_3$	462 [2]	0.320	0.500	0.429
	466 [15]	0.330	0.500	0.429
InTe (L)=InTe (S)	696 [2]	0.500	0.500	
	697 [15]	0.500	0.500	
$L=InTe+In_3Te_4$	649 [2]	0.562	0.510	0.571
	647 [15]	0.550	0.500	0.571
$L+In_2Te_3\beta=In_3Te_4$	650 [2]	0.562	0.595	0.571
	650 [15]	0.560	0.594	0.571
In_2Te_3 (L)$=In_2Te_3\beta$	667 [2]	0.597	0.597	
	669 [15]	0.600	0.600	
$L+In_2Te_3\beta=In_3Te_5\beta$	625 [2]	0.650	0.601	0.625
	625 [15]	0.670	0.609	0.625
$In_2Te_3\beta=In_2Te_3\alpha+In_3Te_5\beta$	615 [2]	0.601	0.600	0.625
	615 [15]	0.605	0.600	0.625
$In_2Te_3\beta=In_2Te_3\alpha$	620 [2]	0.600	0.600	
$In_2Te_3\beta=In_2Te_3\alpha+In_3Te_5\beta$	615 [15]	0.676	0.600	1.000
$In_2Te_3\beta=In_3Te_4+In_2Te_3\alpha$	605 [2]	0596	0.571	0.600
$In_2Te_3\beta+In_3Te_4=In_2Te_3\alpha$	618 [15]	0.601	0.571	0.600
$L+In_3Te_5\beta=In_2Te_5$	467 [2]	0.750	0.625	0.714
	467 [15]	0.760	0.625	0.714
$L+In_2Te_5=Te$	427 [2]	0.900	0.714	1.000
	427 [15]	0.920	0.714	1.000

exhibit extreme behaviour for the same composition which gives indication of a short-range-order based on Tl_2Te associates in the melt.

Nevertheless the phase diagram investigations reveal some uncertainties on the existence of the phase Tl_2Te which appears in the assessment of [2,26] but not in [27,28]. In a very recent work [29] conclude from DSC and X-ray diffraction measurements the existence of the phase Tl_2Te (Fig. 4(d)). Invariant reactions are given in Table 12.

5. Systems Si–, Ge–, Sn–, Pb–Te

5.1. System Si–Te

In the phase diagram presented in Fig. 5(a), Si_2Te_3 has a phase transition according to the structural study of [30] and which is confirmed by the DSC works of [31] who gave 408–410°C as temperature of transition. From these results and new calorimetric investigations of [32], the first results of the thermodynamic optimization led us to propose the invariant reactions reported in Table 13.

5.2. System Ge–Te

The phase diagram (Fig. 5(b)) is characterized by the presence of a solid solution based on the equimolar composition GeTe which undergoes a phase transition cubic→rhombohedral ($\beta\rightarrow\alpha$) in the temperature range 430–405°C and another structural modification cubic→orthorhombic ($\beta\rightarrow\gamma$) in the Te-rich part of the solid solution. On a structural point of view, it is possible to assume that the cubic β form is transformed to α (rhombohedric) by an elongation along a diagonal of the cube, while the $\beta\rightarrow\gamma$ transition is obtained by an elongation of the cube along a crystallographic axis perpendicular to two adjacent faces.

Table 12
Invariant reactions in the system Tl–Te

Reaction	T in °C	Composition of the respective phases in at.% Te		
β-Tl=α-Tl	230 [2]			
	230.0 [27]	0.000	0.000	
	239.9 [29]			
L_1=β-Tl+Tl_2Te	302 [2]	0.005	0.000	0.333
	300.8 [29]	0.005	0.000	0.333
L_1=β-Tl+γ	300.9 [27]	0.014	0.000	0.333
L_2=L_1+Tl_2Te	404 [2]	0.330	0.030	0.333
	407.3 [29]	0.325	0.030	0.333
Tl_2Te (L)=Tl_2Te (S)	425 [2]	0.333	0.333	
	416.2 [29]	0.333	0.333	
L_2=L_1+γ	406.9 [27]	0.298	0.040	0.333
L_2=Tl_2Te+γ	422 [2]	0.337	0.333	0.350
	415.4 [29]	0.335	0.333	0.344
γ (L)=γ (S)	455 [2]	≈0.395	≈0.395	
	452 [27]	0.34	0.34	
	443.0 [29]	0.365	0.365	
γ+L_2=TlTe	300 [2]	0.405	0.580	0.500
	299.9 [27]	0.375	0.535	0.500
	309.9 [29]	0.374	0.531	0.500
TlTe+L_2=Tl_2Te_3	235 [2]	0.500	0.670	0.600
	233.9 [27]	0.500	0.643	0.600
	238.9 [29]	0.500	0.636	0.600
L_2=Tl_2Te_3+Te	224 [2]	0.690	0.600	1.000
	230.9 [27]	0.654	0.600	1.000
	223.9 [29]	0.676	0.600	1.000

Table 13
Invariant reactions in the system Si–Te

Reaction	T in °C	Composition of the respectives phases in at.% Te		
Si+L=Si_2Te_3β	885.0 [2]	0.000	0.620	0.600
	886.1 [in progress]	0.000	0.606	0.600
L=Si_2Te_3β+Te	407.0 [2]	0.850	0.600	1.000
	414.6 [in progress]	0.872	0.600	1.000
Si_2Te_3β=Si_2Te_3α	408.9 [in progress]	0.600	0.600	

Another compound $GeTe_4$ has been found by [33], but DSC and X-ray works of [34,35] led to conclude that it is a metastable phase. The invariant reactions taken from [36,37] are given in Table 14.

Another peculiarity of this system can be found at the Te-rich part in the liquid state. Thermodynamic and physical properties reveal strange temperature dependence around the eutectic composition interpreted as a second order transition [38,39]. From electrical conductivity measurements, [40] interpreted this behaviour as being due to a semiconductor-metal transition associated with destruction of $GeTe_4$ associates.

5.3. System Sn–Te

This system shows a single compound (Fig. 5(c)) of equimolar composition SnTe whose assessed melting point is 806.0°C [2]. The flat part of the liquidus in the metal rich composition corresponds to a tendency to demixing confirmed by the calorimetric results [41–44]. The three thermodynamic evaluations given

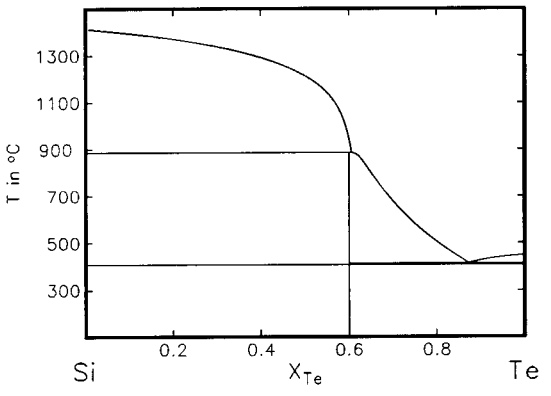

[in progress] 5a

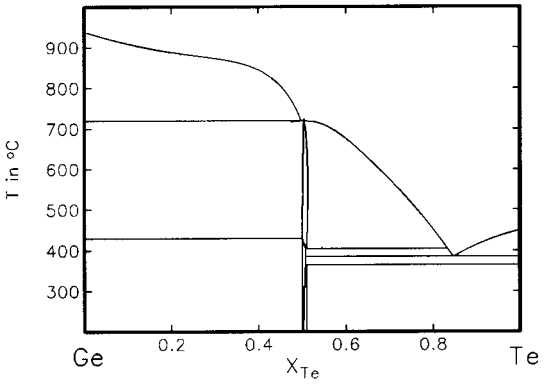

[in progress] 5b

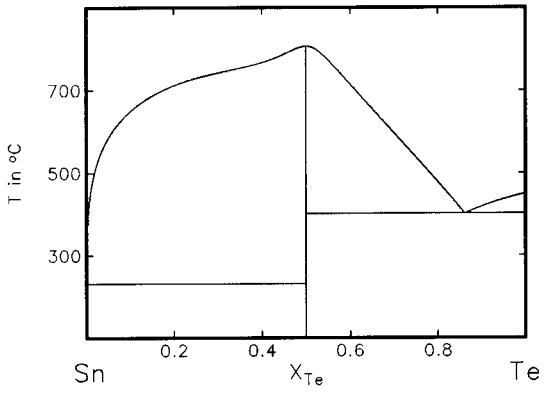

[47] 5c

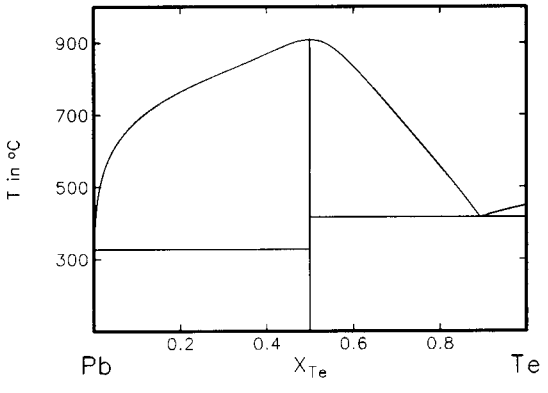

[68] 5d

Fig. 5. Si–, Ge–, Sn–, Pb–Te phase diagram.

by [45–47] are in good agreement (Table 15). Nevertheless [46] described the compound SnTe with a narrow range of homogeneity.

5.4. System Pb–Te

The liquidus in the metal rich side is less flat than in the case of Sn–Te. This may be a consequence of the higher melting point of the equimolar compound PbTe (924°C). However, as shown by the heat of mixing of the melt, a tendency of demixing is still present. The phase diagram is shown in Fig. 5(d). The invariant equilibria are given in Table 16.

6. Systems As–, Sb–, Bi–Te

6.1. System As–Te

The presence of arsenic makes this system very sensitive to pressure variations. In his assessment, [2] proposed a phase diagram (Fig. 6(a)) under pressure high enough to avoid the formation of vapour phase. Thus the phase diagram reports only equilibria between condensed phases. The general shape of the diagram seems to be established. It contains one single intermediate compound (As_2Te_3) with congruent melting (381°C)

Table 14
Invariant reactions in the system Ge–Te

Reaction	T in °C	Composition of the respective phases in at.% Te		
L=Ge+GeTeβ	720 [2]	≈0.500	0.000	≈0.506
	720.0 [in progress]	0.498	0.000	0.505
Ge+GeTeβ=GeTeα	430 [2]	0.000	0.502	0.500
	430.0 [in progress]	0.000	0.501	0.500
GeTe (L)=GeTeβ	724 [2]	0.5061	0.5061	
	724 [37]	0.5061	0.5061	
	720.1 [in progress]	0.506	0.506	
GeTeβ=GeTeα+L	400.0 [2]	0.514	0.830	0.511
	405.0 [37]	0.510	0.830	0.508
	405.0 [in progress]	0.510	0.834	0.508
L=GeTeα+Te	375.0 [2]	0.850	0.508	1.000
	385 [37]	0.850	0.508	1.000
	385.0 [in progress]	0.850	0.508	1.000
GeTeα+Te=GeTeγ	365 [2]	0.509	1.000	0.510
	365.0 [in progress]	0.507	1.000	0.510

Table 15
Invariant reactions in the system Sn–Te

Reaction	T in °C	Composition of the respective phases in at.% Te		
L=Sn+SnTe	231.5 [2]	≈0.01	0.000	0.500
	231.4 [45]	0.000120	0.000	0.500
	232.0 [46]	0.000167	0.000	0.500
	230.2 [47]	0.000138	0.000	0.500
SnTe (L)=SnTe (S)	806 [2]	0.500	0.500	
	808.6 [45][a]	0.500	0.500	
	805.9 [45][a]	0.500	0.500	
	804.2 [46][a]	0.5034	0.5034	
	808.8 [46][a]	0.5048	0.5048	
	807.1 [47]	0.500	0.500	
L=SnTe+Te	401.0 [2]	0.85	0.500	1.000
	399.6 [45]	0.851	0.500	1.000
	401.2 [46]	0.8554	0.500	1.000
	401.5 [47]	0.86	0.500	1.000

[a] Depending on quasi-regular or quasi-sub-regular description of the liquid phase.

Table 16
Invariant reactions in the system Pb–Te

Reaction	T in °C	Composition of the respective phases in at.% Te		
L=Pb+PbTe	326.95 [2]	0.0004	0.000	0.500
	326.91 [68]	0.0010	0.0001	0.500
PbTe (L) = PbTe (S)	924 [2]	0.500	0.500	
	922.7 [68]	0.5001	0.5001	
L=PbTe+Te	410.9 [2]	0.8913	0.500	1.000
	316.14 [68]	0.8926	0.500	1.000

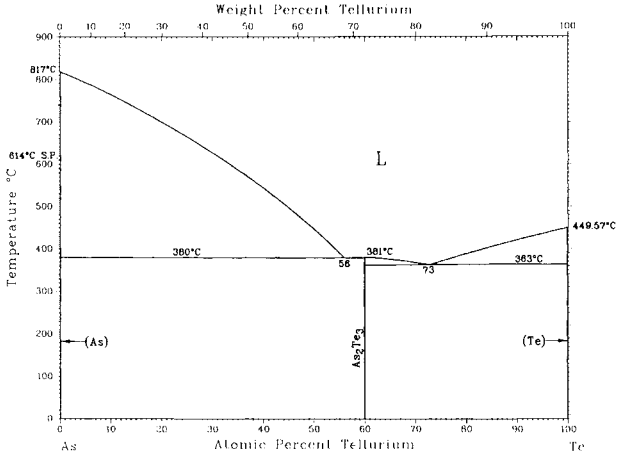

[2] 6a

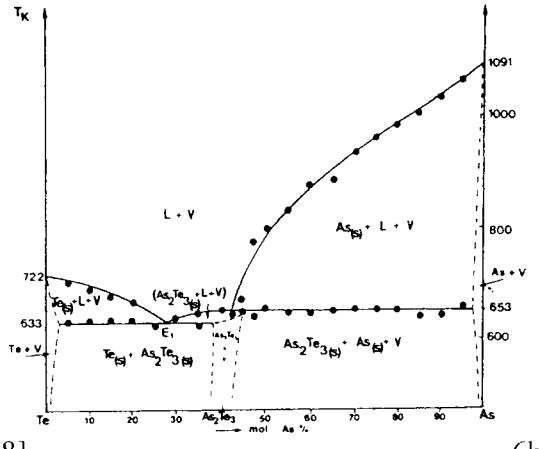

[48] 6b

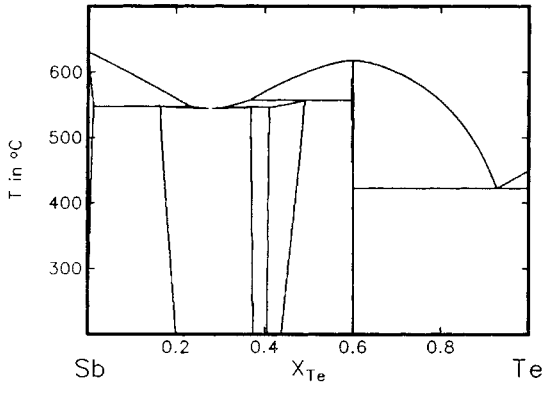

[52] 6c

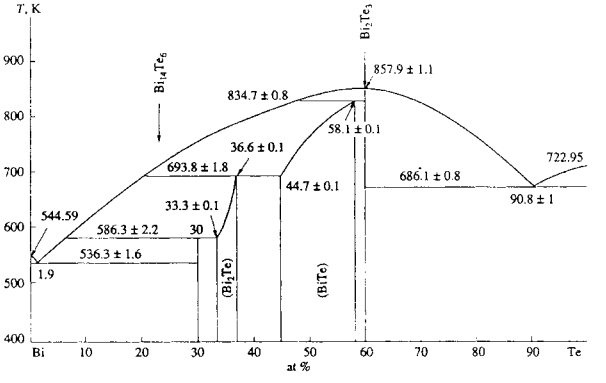

[57, 58] 6d

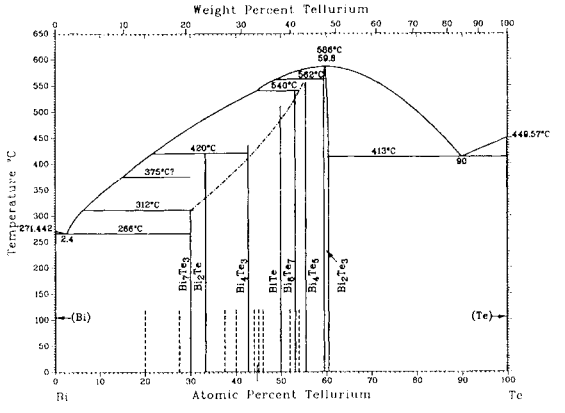

[2] 6e

Fig. 6. As–, Sb–, Bi–Te phase diagram ((a) and (e): courtesy of American Institute of Metals, (b) from [48], (d) from [58]).

Table 17
Invariant reactions in the system As–Te

Reaction	T in °C	Composition of the respective phases in at.% Te		
L=As+As_2Te_3	380 [2]	0.56	0.000	0.600
As_2Te_3 (L)=As_2Te_3 (S)	381 [2]	0.600	0.600	
L=As_2Te_3+Te	363 [2]	0.73	0.600	1.000

and two eutectic invariant equilibria given in Table 17.

In a recent work, [48] considered that the temperature of melting cannot be differentiated from the As-rich side eutectic temperature and presented an isochoric diagram where the specific volume variable is taken into account to explain this anomalous melting. From DTA measurements and electron microprobe analysis on quenched samples, these authors concluded that the melting of As_2Te_3 is non-congruent if the vapour phase is taken into account in the description of the phase equilibria (Fig. 6(b)).

6.2. System Sb–Te

Recent experimental phase diagram investigations were carried out by [49] in the range Sb–Sb_2Te_3 and confirmed the results of [50] except for the temperature of the melting point minimum found at 544°C and 533°C, respectively. Four phases exist in the phase diagram (Fig. 6(c)): Sb_2Te_3 which melts congruently (617.7°C) and has a narrow range of homogeneity (only an alloy with composition $Sb_{0.405}Te_{0.595}$ showed DSC curves with only one thermal arrest corresponding to melting [51]), γ and δ which are solution phases and a terminal solid solution of tellurium in antimony. A thermodynamic evaluation as well as an assessment have been proposed by [52] and [53] respectively. Invariant equilibria reported in both papers are given in Table 18.

New thermodynamic experimental informations should be taken into account in order to improve the description of the Gibbs functions of different phases:

- Heat content measurements of the phase Sb_2Te_3, carried out between 25°C and 649°C showed a second order phase transition [51,54].
- Heat of mixing and chemical potential studies reported for the liquid state in the whole range of concentration [55,56] should allow to obtain more precise entropic coefficients.

6.3. System Bi–Te

The phase diagram knowledge of this system seems to be one of the most difficult to reach among the binaries in this work. Though the different authors agree on the general shape of the liquidus line, the main discrepancy appears about the number and character of the solid phases. Two kinds of phase diagrams may be proposed according to a solution phase description [57,58] (Fig. 6(d)) or stacking variant possibilities [2] (Fig. 6(e)).

Table 18
Invariant reactions in the Sb–Te system

Reaction	T in °C	Composition of the respective phases in at.% Te		
L+Sb=δ	547.5 [2,52,53]	0.231	0.013	0.164
L=δ (minimum)	544.5 [2,52,53]	0.277	0.277	
L+γ=δ	546.0 [2,52,53]	0.308	0.411	0.368
L+Sb_2Te_3=δ	557.2 [2,52,53]	0.367	0.596	0.490
Sb_2Te_3 (L)=Sb_2Te_3 (S)	617.7 [2,52,53]	0.600	0.600	
L=Sb_2Te_3+Te	422.0 [2,52,53]	0.926	0.600	1.000

Characteristics common to both descriptions are:

1. existence of the four phases: Bi_2Te_3, BiTe, Bi_2Te and $Bi_{14}Te_6$.
2. Bi_2Te_3 has a narrow range of homogeneity and melts congruently at 585°C, while the other phases decompose peritectically.
3. agreement on temperature and composition of the eutectic equilibria between Bi and $Bi_{14}Te_6$ and Bi_2Te_3 and Te:

- $L = Bi + Bi_{14}Te_6$ $T = 266°C$ $x^L_{Te} = 0.024$
- $L = Bi_2Te_3 + Te$ $T = 413°C$ $x^L_{Te} = 0.900$

The differences observed between both descriptions come from the fact that structures of all intermediate phases are built from two types of stacking unit, one based on two-layer pure Bi and the other on five-layer Bi_2Te_3 which are stacked along the *c*-axis [59]. These layers may form ordered states at any ratio and only a limited number of structures are experimentally observable. Another kind of explanation has been given by [60] in term of electronic structure. These authors showed a relation between the average number of *p* electrons (electron/atom ratio) and the number of layers in the unit cell. They conclude that for an irrational electron/atom ratio in the range [1/2, 2/3], the *c* parameter of the hexagonal cell would be of an infinite value. This may explain the quasicrystalline character of the phase Bi_8Te_9 reported in [61].

This structural peculiarity allied to difficult in obtaining the equilibrium in the Bi rich side due to slow diffusion which does not allow us to propose a thermodynamic evaluation of the Bi–Te system. Invariant equilibria are reported in Table 19.

7. System Se–Te

This system is apparently the simplest of the post-transitional binaries with tellurium. It is the only one in which neither compound nor invariant reaction appear, just a complete solubility of Te and Se in both liquid and solid state, separated by a two phase field. The temperature of liquidus and solidus have been measured by [62], heat of formation in the liquid has been measured by [62,63] and E.M.F. measurements have been carried out by [64]. A tentative optimization

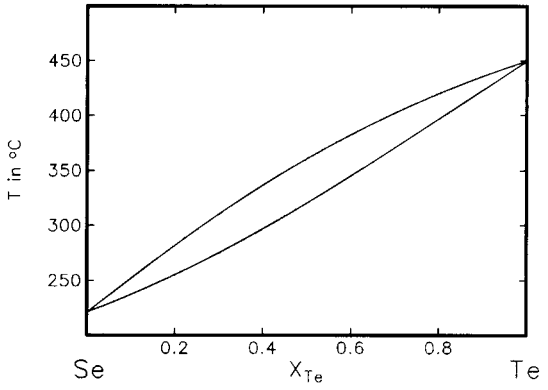

[65]

Fig. 7. Se–Te phase diagram.

Table 19
Invariant reactions in the Bi–Te system

Reaction	T in °C	Composition of the respective phases in at.% Te		
L=Bi+$Bi_{14}Te_6$	266 [2]	0.024	0.000	0.300
	263.2 [58]	0.019	0.000	0.300
L+??=$Bi_{14}Te_6$	312 [2]	0.06	—	0.300
L+Bi_2Te=$Bi_{14}Te_6$	313.2 [2]	0.06	0.0.333	0.3000
L+Bi4Te3=Bi_2Te	420 [2]	0.22	0.429	0.333
L+BiTe=(Bi_2Te)	420.6 [58]	0.22	0.447	0.366
L+??=Bi_6Te_7	540 [2]	0.45	—	0.538
L+(Bi_2Te_3)=(BiTe)	560.9 [58]	0.485	0.597	0.581
L+(Bi_2Te_3)=Bi_4Te_5	562 [2]	0.485	0.597	0.556
(Bi_2Te_3) (L)=(Bi_2Te_3) (S)	586 [2]	0.598	0.598	
	584.8 [58]	0.600	0.600	
L=(Bi_2Te_3)+Te	413 [2]	0.90	0.601	1.000
	413.0 [58]	0.908	0.601	1.000

Table 20
Crystal structure data of stable phases (at 1 bar) P or MC: Powders or Monocrystal, PS: Pearson Symbol, SG: Space Group

Phase	P or MC	PS	SG	Parameters (nm, °)			
				a	*b*	*c*	β
$Cu_{2-x}Te$ a [3]	P	o		0.7319	2.2236	3.6458	
$Cu_{2-x}Te$ b [3]	P	o		1.0186	1.0308	0.4234	
$Cu_{2-x}Te$ c [3]	P						
$Cu_{2-x}Te$ d [3]	P			0.8378		1.0877	
$Cu_{2-x}Te$ f [3]	P	hP22	P3ml	0.8328		0.7219	
$Cu_{2-x}Te$ g [3]	P	m		0.873	1.46	0.719	90.3
$Cu_{2-x}Te$ h [3]	P						
$Cu_{2-x}Te$ i [3]	P						
$Cu_{2-x}Te$ j [3]	P	h		0.853		3.603	
$Cu_{2-x}Te$ k [3]	P	hP6		0.420		0.726	
$Cu_{2-x}Te$ l [3]	P	hP72	P3ml	0.8453		2.1793	
$Cu_{2-x}Te$ l [3]	MC	hP72	P3ml	0.837		2.16	
$Cu_{2-x}Te$ m [3]	P	cF28	$F\bar{4}3M$	0.603			
$Cu_{2-x}Te$ n [71]	MC		Pmnn	0.3991	0.3965	0.6110	
$Cu_{2-x}Te$ p [71]	P	cF28	$F\bar{4}3M$	0.6032			
$Cu_{2-x}Te$ q [71]	P	tP6	P4/nmn	0.398		0.655	
CuTe [71]	MC	oP4	Pmmm	0.316	0.408	0.693	
$Ag_2Te\alpha$ [71]	MC	mPl2	$P2_1/c$	0.809	0.448	0.896	123.33
$Ag_2Te\beta$ [71]	P	cF12		0.657			
$Ag_2Te\gamma$ [71]	P			0.529			
$Ag_{1.9}Te\alpha$ [71]							
$Ag_{1.9}Te\beta$ [71]							
$Ag_5Te_3\alpha$ [71]	MC	hP55	P6/mmm	1.348		0.849	
$Ag_5Te_3\beta$ [71]							
$AuTe_2$ [71]	MC	mC6	C2/m	0.71947	0.44146	0.50703	90.038
ZnTe [71]	MC	cF48	$F\bar{4}3m$	0.61026			
CdTe [71]	P	cF8	$F\bar{4}3m$	0.6481			
HgTe [71]	P	cF8	$F\bar{4}3m$	0.6458			
Al_7Te_{10} [71]	MC	hR34	R32	1.4395		1.7932	
GaTe [71]	MC	mC24	C2/m	1.7404	0.4077	1.7930	145.61
Ga_2Te_3 [71]	P	cF8	$F\bar{4}3m$	0.5892			
Ga_3Te_4 [71]	P	hP		0.8278		0.6906	
Ga_2Te_5 [71]	MC	tI14	I4/m	0.7913		0.6848	
In_4Te_3 [71]	MC	oP28	Pnnm	1.5630	1.2736	0.4441	
InTe [71]	MC	tI16	I4/mcm	0.8454		0.7152	
In_3Te_4 [71]	MC	hR7	$R\bar{3}m$	0.427		4.09	
$In_2Te_3\alpha$ [71]	MC	cF8	$F\bar{4}3m$	1.850			
$In_2Te_3\beta$ [71]	P	cF8	$F\bar{4}3m$	0.616			
$In_3Te_5\alpha$ [71]	P	hP		1.327		0.356	
$In_3Te_5\beta$ [71]							
In_2Te_5 [71]	MC	mC28	Cc	0.439	1.639	1.352	91.65
TlTe [71]	MC	tI32	I4/mcm	1.295		0.618	
Tl_2Te_3 [71]	MC	mC20	Cc	1.7413	0.6552	0.7910	133.16
Tl_5Te_3 [71]	MC	tI32	I4/mcm	0.8930		1.2589	
Tl_2Te [29]							
Si_2Te_3 [71]	MC	hP40	P31c	0.74223		1.34647	
$GeTe\alpha$ [71]	P	hR2	R3m	0.847		1.038	
$GeTe\beta$ [71]	P	cF8	$Fm\bar{3}m$	0.600			
$GeTe\gamma$ [71]	P	oP8	Pnma	1.176	0.415	0.436	
SnTe [71]	P	cF8	$Fm\bar{3}m$	0.6320			
PbTe [71]	MC	cF8	$Fm\bar{3}m$	0.6462			

Table 20 (continued)

Phase	P or MC	PS	SG	Parameters (nm, °)			
				a	*b*	*c*	β
AsTe [71]	P	cF8	$Fm\bar{3}m$	0.5778			
Sb_2Te_3 [71]	P	hR5	$R\bar{3}m$	0.4264		3.0458	
SbTe [71]	P	hP12	$P\bar{3}ml$	0.426		2.39	
BiTe [71]	MC		$P\bar{3}ml$	0.44232		2.40026	
Bi_4Te_3 [72]	MC		$R\bar{3}m$	0.44511		4.18885	
Bi_2Te_3 [61]	MC		$R\bar{3}m$	0.43953		3.0441	
Bi_9Te_{11} [71]	P	h		0.442144		7.819512	
$Bi_{43}Te_{57}$ [71]	P	h		0.441062		5.43303	

has been performed by [65] though he had not all thermodynamic data at that time. In a compilation, the same author [66] recognized that the model used to describe the liquid state in the optimization was not suitable. Recently [67], proposed the RMMC (Regular Model with Multiple Connectivity) model for the liquid state in the diagram.

The model is based on the following observations. Se in the liquid state is a semiconductor and tellurium is metallic. In the liquid state selenium is two fold coordinated and in tellurium coexist metallic three fold coordinated and semiconducting two fold coordinated microdomains (Te^{II} and Te^{III}). The Se–Te system in the liquid state in now considered as a ternary system with Se, Te^{II} and Te^{III}.

From this model, heat of formation and Gibbs function (free enthalpy) are recalculated, the values are in a very good agreement with the experimental values of [64] for Gibbs function and [62] for the enthalpies of mixing. The Se–Te binary is presented in Fig. 7.

This model is particularly important, because in a lot of applications it is necessary to use multicomponent alloys including selenium, tellurium and other metals. The investigation of this kind of systems is too long using X-ray and thermal analysis, the combination of experiments and calculation resulting in optimization should allow to solve phase diagrams of higher order alloys system (after compatibility between the formalism of RMMC and the available calculation softwares).

8. Conclusion

The binaries between tellurium and post-transitional elements with a metallic character give intermediate compounds (structural information is given in Table 20) and in a great number of cases, these compounds have phases transitions.

Moreover, in many cases, we observe a liquid–liquid miscibility gap, or a tendency to have it. With Se, we obtain only a solid solution separated from the liquid by a two phase field.

The liquid phase, in most of cases, shows the existence of associate. On a thermodynamic point of view, it can be described either with an association model or a partially ionic model. In all the cases in the calculation the gas phase must be taken into account, because its influence may be drastic for the preparation of compounds.

References

[1] A.T. Dinsdale, CALPHAD 15 (1991) 317.
[2] T.B. Massalski, Binary Alloy Phase Diagram, 2nd ed., Vol. 1, 2, 3, ASM International, Materials Park, OH, 1990.
[3] R. Blachnik, M. Lasoka, P. Walbrecht, J. Sol. State Chem. 48 (1983) 431.
[4] F.C. Kracek, C.J. Ksanda, L.J. Cabri, Am. Mineral. 51 (1966) 14.
[5] R. Castanet, Y. Claire, M. Laffitte, J. Chim. Phys. 68 (1971) 1133.
[6] R. Castanet, M. Laffitte, Rev. Int. Hautes Temp. Refract. 11 (1974) 103.
[7] R. Castanet, C. Bergman, J. Chem. Thermodyn. 11 (1979) 83.
[8] T. Maekawa, T. Yokokawa, J. Chem. Thermodyn. 7 (1975) 505.
[9] Y. Feutelais, D. Mouani, J.-R. Didry, B. Legendre, J. Phase Equilib. 15 (1994) 380.
[10] F. Sommer, Z. Metallkd. 73 (1982) 72.
[11] F. Sommer, Z. Metallkd. 73 (1982) 77.
[12] Y. Feutelais, A. Haloui, B. Legendre, J. Phase Equilib. 18 (1997) 48.
[13] Y. Feutelais, B. Legendre, S. Robert, J.-C. Tedenac, 24th. CALPHAD Conference, Kyoto, 1995.

[14] H. Said, R. Chastel, C. Bergmann, R. Castanet, Z. Metallkd. 72 (1981) 360.
[15] Chang-Seok Oh, Dong Nyung Lee, CALPHAD 17 (1993) 175.
[16] M. Hillert, B. Jansson, B. Sundman, J. Agren, Metall. Trans. A 16A (1985) 261.
[17] R. Blachnik, E. Irle, J. Less-Common Met. 113 (1985) L1.
[18] E. Irle, B. Gather, R. Blachnik, U. Kattner, H.-L. Lukas, G. Petzow, Z. Metallkd. 78 (1987) 535.
[19] Chang-Seok Oh, Dong Nyung Lee, CALPHAD 16 (1992) 317.
[20] D. Mouani, G. Morgant, B. Legendre, J. Alloys Comp. 226 (1995) 222.
[21] J.H.C. Hogg, H.H. Sutherland, Acta Crystallogr. B 29 (1973) 2483.
[22] H. Said, M.L. Michel, R. Castanet, J. Calorim. Anal. Therm. 8 (1977) 87.
[23] H. Said, R. Castanet, J. Calorim. Anal. Therm. B 9 (1978) 171.
[24] H. Said, R. Castanet, High Temp.-High Pres. 10 (1978) 681.
[25] H. Said, R. Castanet, High Temp.-High Press. 11 (1979) 343.
[26] H. Okamoto, J. Phase Equilib. 12 (1991) 507.
[27] Chang-Seok Oh, Dong Nyung Lee, J. Phase Equilib. 14 (1993) 197.
[28] H. Okamoto, J. Phase Equilib. 15 (1994) 131.
[29] M.-C. Record, Y. Feutelais, H.-L. Lukas, Z. Metallkd. 88 (1997) 45.
[30] P.E. Gregoriades, G.L. Bleris, J. Stoemenos, Acta Crystallogr. B 39 (1983) 421.
[31] I.N. Odin, V.A. Ivanov, Russ. J. Inorg. Chem., 36 (1991) 749; Zh. Neorg. Khim., 36 (1991) 1314.
[32] A. Schlieper, R. Blachnik, J. Alloys Comp. 235 (1996) 237.
[33] A.G. Moore, C. Maghrabi, J.M. Parker, J. Mater. Sci. 13 (1978) 1127.
[34] S. Asokan, G. Parthasarathy, E.S.R. Gopal, Mat. Res. Bull. 21 (1986) 217.
[35] A. Schlieper, PhD, University Osnabrück, Germany, 1996.
[36] B. Legendre, C. Souleau, C.R. Acad. Sci. Paris, Sér. C 284 (1977) 315.
[37] B. Legendre, C. Hancheng, S. Bordas, M.T. Clavaguera-Mora, Thermochim. Acta 78 (1984) 141.
[38] R. Castanet, C. Bergman, Phys. Chem. Liq. 14 (1985) 219.
[39] Y. Tsuchiya, J. Non-Crystall. Sol. 156–158 (1993) 704.
[40] Y. Tsuchiya, H. Saitoh, J. Phys. Soc. Jap. 62 (1993) 1272.
[41] M. Le Boutelier, A.M. Martre, R. Fahri, C. Petot, Metall. Trans. B 8B (1977) 339.
[42] Y. Nakamura, S. Himuro, M. Shimoji, Ber. Bunsenges. 84 (1980) 240.
[43] J. Rakotomavo, M.-C. Baron, C. Petot, Metall. Trans. B 12B (1981) 461.
[44] R. Blachnik, B. Gather, Z. Metallkd. 74 (1983) 172.
[45] K.-C. Hsieh, M.S. Wei, Y.A. Chang, Z. Metallkd. 74 (1983) 330.
[46] U. Kattner, H.-L. Lukas, G. Petzow, J. Less-Common Met. 114 (1985) 129.
[47] M.T. Clavaguera-Mora, C. Comas, N. Clavaguera, CALPHAD 18 (1994) 141.
[48] J.-C. Rouland, R. Ollitrault-Fichet, J. Flahaut, J. Rivet, R. Céolin, Thermochim. Acta 161 (1990) 189.
[49] S. Bordas, M.T. Clavaguera-Mora, B. Legendre, C. Hancheng, Thermochim. Acta 107 (1986) 239.
[50] N.Kh. Abrikosov, L.V. Poretskaya, I.P. Ivanova, Russ. J. Inorg. Chem. 4 (1959) 1163; Zh. Neorg. Khim. 4 (1959) 2525.
[51] B. Legendre, Y. Feutelais, J.-R. Didry, J. Therm. Anal. 34 (1988) 345.
[52] G. Ghosh, H.-L. Lukas, L. Delaey, Z. Metallkd. 80 (1989) 731.
[53] G. Ghosh, J. Phase Equilib. 15 (1994) 349.
[54] Y. Feutelais, N.B. Chanh, B. Legendre, J.-R. Didry, J. Therm. Anal. 35 (1989) 2423.
[55] Y. Feutelais, B. Legendre, G. Morgant, J. Therm. Anal. 34 (1988) 345.
[56] Y. Feutelais, B. Legendre, S. Misra, T. Anderson, J. Phase Equilib. 15 (1994) 171.
[57] N.Kh. Abrikosov, V.F. Bankina, Russ. J. Inorg. Chem. 3 (1958) 152; Zh. Neorg. Khim. 3 (1958) 659.
[58] S.N. Chizhevskaya, L.E. Shelimova, V.S. Zemskov, V.I. Kosyakov, D.V. Malakhov, Inorg. Mater. 30 (1994) 1; Neorg. Mater. 30 (1994) 3.
[59] P.M. Imamov, S.A. Semiletov, Sov. Phys. Crystall. 15 (1971) 845; Kristallografiya. 15 (1970) 972.
[60] J.-P. Gaspard, R. Ceolin, Sol. State Comm. 84 (1992) 839.
[61] Y. Feutelais, B. Legendre, N. Rodier, V. Agafonov, Mat. Res. Bull. 28 (1993) 591.
[62] G. Morgant, B. Legendre, J. Therm. Anal. 31 (1986) 377.
[63] T. Maekawa, T. Yokokawa, K. Niwa, Bull. Chem. Soc. Japan. 46 (1973) 761.
[64] N. Mouloudj, C. Petot-Ervas, C. Petot, B. Legendre, Thermochim. Acta 136 (1988) 87.
[65] G. Ghosh, H.-L. Lukas, L. Delaey, CALPHAD 12 (1988) 295.
[66] G. Ghosh, R.C. Sharma, D.T. Li, Y.A. Chang, J. Phase Equilib. 15 (1994) 213.
[67] A. Amzil, M. Gilbert, C. Bichara, J.-C. Mathieu, J. Phys. Cond. Mat. 8 (1996) 5281.
[68] U. Kattner, H.-L. Lukas, G. Petzow, CALPHAD 10 (1986) 103.
[69] Yang Jianrong, N.J. Silk, A. Watson, A.W. Bryant, B.B. Argent, CALPHAD 19 (1995) 339.
[70] H. Okamoto, T.B. Massalski, Bull. Alloy Phase Diagr. 5 (1984) 172.
[71] P. Villars, L.D. Calvert, Pearson's handbook of Crystallographic Data for Intermetallic Phases, 2nd ed., Vol. 1, 2, 3, 4, ASM International, Materials Park, OH, 1991.
[72] K. Yamana, K. Kihara, T. Matsumoto, Acta Crystallogr. B 35 (1979) 147.